IC/97/32

INTERNATIONAL CENTRE FOR
THEORETICAL PHYSICS

THE NONMETAL-METAL TRANSITION IN SOLUTIONS OF METALS IN MOLTEN SALTS

M.P. Tosi

INTERNATIONAL
ATOMIC ENERGY
AGENCY

UNITED NATIONS
EDUCATIONAL,
SCIENTIFIC
AND CULTURAL
ORGANIZATION

IC/97/32

United Nations Educational Scientific and Cultural Organization
and
International Atomic Energy Agency

INTERNATIONAL CENTRE FOR THEORETICAL PHYSICS

THE NONMETAL-METAL TRANSITION IN SOLUTIONS OF METALS IN MOLTEN SALTS

M.P. Tosi *
International Centre for Theoretical Physics, Trieste, Italy.

ABSTRACT

Solutions of metals in molten salts present a rich phenomenology: localisation of electrons in disordered ionic media, activated electron transport increasing with metal concentration towards a nonmetal-metal (NM-M) transition, and liquid-liquid phase separation. A brief review of progress in the study of these systems is given in this article, with main focus on the NM-M transition. After recalling the known NM-M behaviour of the component elements in the case of expanded fluid alkali metals and mercury and of solid halogens under pressure, the article focuses on liquid metal - molten salt solutions and traces the different NM-M behaviours of the alkalis in their halides and of metals added to polyvalent metal halides.

MIRAMARE - TRIESTE
April 1997

* Permanent address: Istituto Nazionale di Fisica della Materia e Classe di Scienze, Scuola Normale Superiore, Piazza dei Cavalieri 7, I-56126 Pisa, Italy.

1. Background and outline

Solutions of metals in molten salts are among the classes of systems which undergo a transition from a nonmetallic to a metallic state on changing some thermodynamic variable. Early work on phase diagrams and electrical transport, which is summarised in the reviews of Bredig[1] and Corbett[2], established that upon dissolving a metal in its molten halide a true solution is formed on a microscopic scale rather than a suspension of colloidal particles of metal, and showed a continuous increase in electrical conductivity from the purely ionic to the metallic regime at high enough temperature. The manner in which the change from localised to extended electronic states occurs is a problem of great general interest[3-5].

In the salt-rich regime the added metal atoms are ionised and their valence electrons can be accommodated inside the structure of the liquid host when the solvent is a molten alkali halide. In the case of polyvalent metal halides the transfer of these electrons to the cations of the host may instead lead to formation of cationic species of intermediate valence or polyatomic cationic species in "subhalide" compounds. In either case thermally activated electron transport and the evolution of liquid structure with composition eventually develop into a nonmetal-metal (NM-M) transition. Figure 1 reports the phase diagram of the cesium-iodine system, together with data showing the dependence of the electrical conductivity on composition. This is an especially simple example, insofar as complete solubility occurs at all temperatures above the liquidus. The lighter alkali systems instead show a wide range of liquid-liquid immiscibility culminating in a critical consolute temperature. In polyvalent metal systems the stability of mixed-valence or polyatomic subhalide species may further enrich the phase diagram and shift the miscibility gap into the metal-rich regime and the critical point to very high temperatures.

As to the content of this review, it will be useful to set the scene to NM-M transitions in these solutions by a brief survey in § 2 of the NM-M behaviour of the component elements. A great deal of detailed evidence is now available on NM-M transitions exhibited by the heavier alkali metals and by mercury on the liquid-vapour coexistence curve and by the solid molecular halogens under pressure. The evidence on the evolution of electronic states with concentration in alkali - alkali halide solutions will be reviewed in § 3, starting from the state of a single solvated electron and up to the NM-M transition and the critical miscibility behaviour. The main emphasis in § 4 will be on

Bi - Bi halides and on Na - cryolite solutions as illustrative systems for polyvalent metals, the former being a paradigm of complex phase behaviour due to the stability of polyatomic cations and the latter a system of great practical relevance in relation to industrial processes for the production of Al metal. The article concludes with a brief summary in § 5.

2. The nonmetal-metal behaviours of the component elements

2.1 Expanded fluid alkali metals

The possibility of separate first-order electronic and liquid-vapour transitions in fluid metals was suggested a long time ago by Landau and Zeldovitch[6]. Although a clear-cut answer to this question is as yet not available, the study of fluid Rb and Cs in the liquid-vapour critical region has led to remarkable progress in understanding[7, 8]. The critical data of these metals are T_c = 2017 K, p_c = 12.45 MPa and d_c = 0.292 g cm^{-3} for Rb and 1924 K, 9.25 MPa and 0.379 g cm^{-3} for Cs.

The main experimental approaches have involved the determination of the equation of state, the electrical conductivity and the thermopower, the magnetic susceptibility and the Knight shift, the optical reflectivity and the dielectric function. The shape of the coexistence curves of these liquid metals and their vapours is very different from those of insulating monatomic fluids, owing to strong deviations from the empirical law of rectilinear diameter. The studies of electronic properties show that, starting from a nearly-free-electron liquid metal near the triple point, strong electron-electron correlations emerge as the critical point is approached from the liquid side. On the vapour side, a large amount of diamagnetic units such as the molecular dimer and probably larger clusters are present in the critical region.

Neutron diffraction data on the liquid structure factor for these metals expanded by heating towards their critical points have been used by Hensel and coworkers[8] to derive the characteristic changes in the microscopic structure and in particular the near-neighbour distance and the coordination number as functions of density. The lowering of the density is associated with only a very slight growth of the near-neighbour distance and hence mostly occurs through a depletion of the first-neighbour shell around each atom. These observations indicate that a chemical bond is emerging as the basic building block in the expanded fluid states. Further relevant evidence comes from inelastic

neutron scattering measurements of the dynamic structure factor of liquid Rb, with results which are consistent with the emergence of optic-type modes in the NM-M transition range.

In summary, the data seem to suggest that a conducting state is preserved in the liquid heavy alkalis on the approach to the critical point through the persistence of "filamentary" structures stabilised by chemical bonding and probably in coexistence with small clusters such as the ionised dimer. These structures evolve into molecular groups on the vapour side of the critical point.

2.2 Expanded fluid mercury and dense mercury vapours

Extensive studies of the approach to the critical region have also been carried out for fluid Hg[9,10].The critical data are T_c = 1751 K, p_c = 167 MPa and d_c = 5.8 g cm^{-3}. The measured Knight shift, which is proportional to the *s*-electron density of states at the Fermi level, vanishes near 9 g cm^{-3}. From optical absorption data, a gap in the density of states opens up at about the same density. This type of metal-semiconductor transition is predicted by standard band theory for an expanded divalent metal when the 6*s* and 6*p* conduction bands no longer overlap, the role of liquid-state disorder being apparently limited to a smearing out of the band edges.

From energy dispersive X-ray diffraction measurements[11] the near-neighbour distance in the liquid metal is nearly independent of density, while the average coordination number decreases almost linearly with density. However, this structural trend changes as the transition is approached: in particular, the average near-neighbour distance starts to gradually increase and eventually approaches in the insulating vapour phase the value of the equilibrium distance in the weakly attractive van der Waals potential of the Hg dimer.

Studies of the ionisation threshold in clusters as a function of the cluster size show qualitatively the same behaviour for Hg as for the insulating rare-gas elements in the small-cluster regime[9]. However, the threshold drops by more than 2 eV for Hg clusters in the size region between about 13 and 100 atoms, eventually approaching the behaviour calculated for ideally conducting spheres. All the evidence shows that profound changes in the electronic structure of small Hg clusters are taking place with increasing size. The appearance of large charged droplets in the vapour near saturation and in supercritical fluid Hg has been proposed from the observed behaviour of the sound velocity over broad ranges of temperature and pressure[12].

2.3 Solid halogens under pressure

Pioneering work on the properties of solid molecular I_2 under pressure was carried out by Drickamer and coworkers[13]. The electrical resistance decreases drastically with increasing pressure and exhibits metallic behaviour at about 20 GPa. In measurements of optical absorption the optical gap tends to zero at around 16 GPa. Subsequent experiments[14] using X-rays showed that the molecular structure persists up to about 20 GPa.

Pasternak *et al.*[15] studied the ^{129}I Mössbauer effect in the solid under pressure at 4 K and reported the formation of I_2-I_2 zig-zag chains above 16 GPa and of a quasi two-dimensional structure above 21 GPa. In *ab initio* molecular dynamics studies of high-density hydrogen Hohl *et al.*[16] have proposed a similar two-stage transformation: under pressure the diatomic molecules line up to form filaments and these order into layers upon further application of pressure at low thermal energies, the intermolecular distances becoming comparable with the bond length in the molecule.

Very recently Fujihisa *et al.*[17] have performed structural studies of solid Br_2 subjected to high pressure up to 80 GPa, where this solid exhibits a molecular to monatomic phase transition. By combining data for I_2, Br_2 and Cl_2 these authors point out that a scaling rule involving the molecular bond length R_b is obeyed in the three isostructural halogens: molecular dissociation occurs at the critical scaled volume $\tilde{v}_c = 1.29$, the scaled volume being defined as $\tilde{v} = v/8R_b^3$ where v is the unit cell volume. They also evaluate the molar refractivity R as a function of pressure from the measured unit cell volume and point out that $R = 1$ at $\tilde{v}_c = 1.29$. Use of the Herzfeld criterion[18] then suggests that metallization under pressure is related to molecular dissociation in these elemental solids. The molar refractivity $R(\omega)$ at frequency ω is related to the real part $\varepsilon_1(\omega)$ of the dielectric function by

$$\frac{\varepsilon_1(\omega)-1}{\varepsilon_1(\omega)+2} = R(\omega) \quad . \tag{1}$$

According to the Herzfeld criterion the *static* dielectric constant diverges at the NM-M transition, which corresponds to $R(0) = 1$.

3. Solutions of alkali metals in their halides

3.1 Structure of molten alkali halides

The main characteristic feature of short-range order in molten salts near freezing at standard

pressure is the preservation of the alternation of positively charged and negatively charged species in space. This type of chemical order due to Coulomb interactions in the melt is illustrated in Figure 2, which collects the results on the partial pair distribution functions $g_{\alpha\beta}(r)$ in molten NaCl at 875 °C from neutron diffraction experiments by the isotope enrichment technique, from classical computer simulation and from pair-potentials theory[19]. The definition of $g_{\alpha\beta}(r)$ is such that the quantity $4\pi r^2 n_\beta g_{\alpha\beta}(r)dr$ gives the average number of β-type ions lying in a spherical shell of radius r and thickness dr centred on an α–type ion, $n\beta$ being the number density of β–type ions. The data in figure 2 are representative of the structural ordering in other molten alkali halides, with the possible exception of Li halides.

It is evident from figure 2 that Coulomb attractions and closed-shell overlap repulsions between Na^+ and Cl^- ions lead to a first-neighbour shell of unlike ions around any given ion, with a sharply defined region of excluded volume. The Coulomb repulsions between like (Na^+-Na^+ or Cl^--Cl^-) ions push them into second-neighbour shells that have similar shapes and show less sharply defined regions of excluded volume. Alternation of the two ionic species in space is clearly preserved to a great extent across melting, so that the distribution of charge density around any given ion has an oscillatory profile.

In spite of the large volume expansion of NaCl on melting ($\Delta V/V_{liq} \approx 0.28$) the average first-neighbour bond length in the melt, as given by the position of the main peak in $g_{+-}(r)$, is somewhat shorter than the first-neighbour distance in the crystal before melting (2.78 Å against 2.95 Å). In fact, the main peak in $g_{+-}(r)$ is asymmetrically broadened, making it difficult to give a precise assessment of the average first-neighbour coordination number in the melt. It is nevertheless clear that the coordination is somewhat lower than the value 6 appropriate to the NaCl crystal.

Figure 2 also shows that the main minimum in $g_{+-}(r)$ is fairly deep, suggesting a moderate rate of ionic exchange between the first-neighbour shell and the surrounding liquid. The estimated persistence times of local structure in molten alkali halides near freezing are of the order of several picoseconds[20]. These correspond to values of the ionic conductivity $\sigma = 3.6\ \Omega^{-1}\ cm^{-1}$ and of the shear viscosity $\eta = 1.0$ cp in molten NaCl near freezing, which are typical of strongly ionic melts. The self-diffusion coefficients of the two ions in NaCl have similar values ($D_{Na} = 1.7$ and $D_{Cl} = 1.3\times10^{-4}\ cm^2\ s^{-1}$), in spite of the large differences in ionic radii and ionic masses: this is consistent

with the observed similarity between $g_{++}(r)$ and $g_{--}(r)$ in Figure 2, which implies similarity in restoring forces and residence times for the two ionic species[21]. The reader is referred to the review of Rovere and Tosi[5] for discussions of how Coulomb ordering affects various other dynamical properties of ionic melts.

In the presence of an oscillatory character of the screening charge density as already remarked above, a useful definition of the ionic screening length in a molten salt can be obtained from the Debye-Hückel concept of the potential drop across the dipole layer formed by any given ion and by the charge distribution surrounding it. The relevant thermodynamic quantity is the Coulombic internal energy U_C of the melt. A simple and physically transparent analytic result can be given for a 1:1 melt in the primitive model of equi-sized charged hard spheres as solved in the so-called mean spherical approximation. This yields

$$U_C = -\frac{e^2}{L_1 + \sigma/2} \tag{2}$$

where σ is the sum of the two ionic radii and

$$L_1 = \sigma[(1+\frac{2\sigma}{L_D})^{1/2} - 1]^{-1} \quad , \tag{3}$$

$L_D = (4\pi ne^2 / k_B T)^{-1/2}$ being the Debye-Hückel length. The length L_i can be identified with the ionic screening length in the molten salt. More generally, this line of argument leads to an expression for the ionic screening length which is a function of density, temperature, core dielectric constant, ionic charges and ionic radii, allowing contact to be made with data on the differential capacitance of electrode/molten salt interfaces[22].

3.2 The solvated electron

Alkali halide crystals are coloured in the visible by the addition of minute quantities of alkali metal: the metal dissociates into positive ions and electrons and the latter are trapped at negative ion vacancies forming F centres. The optical absorption associated with F centres was followed across melting in the early work of Mollwo[23]. A broad red-shifted band is observed in the melt, the peak frequency E_m being related to that in the crystal through the volume V by the empirical Mollwo-Ivey law $E_m \propto V^{-2/3}$[24]. This law is, of course, suggestive of electron confinement inside a box.

Magnetic resonance experiments provide further evidence for the existence of a liquid-state analogue of the crystalline F centre. Electron residence times of the order of 10^{-12} s (of the same order

as the time of persistence of local ionic structures in the melt - see § 3.1) have been estimated from measured nuclear relaxation rates and shown to be consistent with transport measurements of the electron mobility[25]. ESR measurements[26, 27] yield values of the *g* factor in several dilute liquid mixtures which are quite close to those observed for F centre resonances in the corresponding crystals. The observed resonances in the liquid are appreciably narrower, however, suggesting fast diffusional or exchange processes.

According to both theory[28] and quantal computer simulations[29, 30] the localised state for a single electron in a molten alkali halide partakes of F-centre and polaron character, in the sense that localisation occurs at favourable structural fluctuations with the help of a local cooperative rearrangement of the ions. With reference to molten KCl as a typical host, the local structure around the trapped electron is found to consist of about four alkali ions on average, which produce a depth of 3-4 eV for the trapping well and bind the electron by 2-2.5 eV. The root mean square radius of the electron cloud is about 2-2.5 Å, confirming that the diamagnetic contribution is only a fraction (10-20%) of the measured excess magnetic susceptibility. The contact values of the electron density at the nuclei in molten CsCl (3 $Å^{-3}$ at the Cs nucleus and 0.04 $Å^{-3}$ at the Cl one) are of the same order as reported from measurements of NMR hyperfine shifts. There also is quite satisfactory agreement between theory and experiment for what concerns the peak frequency and the band width of the optical absorption associated with transitions of the localised electron to excited states.

3.3 The salt-rich region and the nonmetal-metal transition

Magnetic resonance and optical absorption measurements have also been used to follow the evolution of the nature of electron localisation with increasing concentration *c* of added metal in molten alkali halides. The optical absorption spectrum shows great sensitivity to the content of added metal, reflecting aggregation phenomena which seem to start at very low metal content (less than 0.01 mol) and progressively reduce the fraction of added electrons which are localised in F-centre-like states[24,31]. The emergence of a new absorption band at $c = 0.19$, red-shifted by almost 1 eV relative to the F-centre band, is suggestive of the formation of small metal clusters[32]. The absorption associated with F-centre electrons is still present, however.

The ESR measurements[26, 27] show a decreasing relative weight of unpaired spin densities with increasing concentration of metal and the emergence of a new resonance which is attributed

to electrons localised in small clusters. The molar magnetic susceptibility of the dissolved metal in several molten salts approaches the bulk value of the pure metal at $c \approx 0.2$.

The aforementioned evidence thus indicates that with increasing c the single-electron localised states are still present but coexist with spin-paired electron states and with small fluctuating clusters of metal. The approach to the NM-M transition in K_c-KCl_{1-c} is most strikingly signalled by a dielectric anomaly[32]: the real part of the dielectric function measured at a wavelength of 2.316 μm and at 800 °C shows a strong maximum at $c \approx 0.25$. According to the Herzfeld criterion the *static* dielectric constant should diverge at the NM-M transition (see § 2.3). At finite temperatures and frequencies no such divergence can be expected, but a pronounced change in the real part of the low-frequency dielectric function as a function of composition may still be indicative. The observed dielectric anomaly therefore seems to locate the NM-M region in the range $0.2 \leq c \leq 0.3$ for the K_c-KCl_{1-c} system. It should be emphasised that this metal content is well below that at the critical point for demixing, which lies at $c = 0.39$ and T = 790 °C in this system (see § 3.4 below).

The evidence reviewed above seems still insufficient to attribute a specific type (Anderson, Mott-Hubbard or percolation) to the NM-M transition in metal - molten salt solutions. A dielectric anomaly does not *per se* identify the microscopic nature of the transition. The evidence for spin pairing with increasing metal content suggests a similarity with metal-ammonia solutions, molecular dimers being one of the basic ingredients in the picture that Mott[3] has given for the NM-M transition as it occurs in these systems. He proposed that the transition arises from the crossing of two bands as the metal content increases - one band for an extra electron on a dimer and the other for a hole in a dimer. On the other hand, if larger clusters form in a microscopically inhomogeneous regime preceding the transition, a volume percolation mechanism as introduced for some metal-ammonia solutions by Webman *et al.*[33] could be an alternative to a Mott-Hubbard mechanism. Senatore and Tosi[34] have evaluated a percolation model showing that it yields a critical metal concentration of ≈ 0.2-0.25 for the NM-M transition in potassium - potassium halide solutions.

I have already remarked that the basic F-centre-like localised state coexists with higher clusters as the metal content is increased. Turning to the stability of this state, it was recently noticed by Yurdabak *et al.*[35] that, as electrons are released into conduction states because of natural limitations

on the number of available localisation sites, the onset of metallic screening would lead to an abrupt collective transition of the valence electron assembly to a metallic state. This argument, combined with the evidence from computer simulation recalled in § 3.2 above on fourfold coordination for the solvated electron, locates the NM-M transition at $c \approx 0.25$.

Akdeniz and Tosi[36] have further developed this model by introducing some allowance for a finite lifetime of the localisation clusters, due to thermally activated electron hopping and for their evolution with composition. This was done through an electronic screening length L_e which allows both for Thomas-Fermi screening from electrons in conduction states and for screening by hopping electrons over a distance of the order of the mean distance between occupied localisation sites. Namely,

$$L_e = [xL_h^{-2} + (1-x)L_{TF}^{-2}]^{-1/2} \qquad (4)$$

where cx is the molar fraction of F-centre electrons and

$$L_h = \alpha(\pi cx / 6v)^{-1/3} \quad , \qquad (5)$$

$$L_{TF} = L_o[c(1-x)v_K / v]^{-1/6} \qquad (6)$$

with v the molar volume, v_K the partial molar volume of the cation, L_o the Thomas-Fermi length of the pure metal and $\alpha \approx 1/4$. In determining the equilibrium value of x at each value of c, account was also taken of ionic screening as discussed in § 3.1. This model leads to a *continuous* progressive dissolution of the localisation centres and hence to a smooth transition to the metallic state, occurring at a critical metal content of 0.25-0.30 in K-KCl at 800 °C.

3.4 Critical concentration fluctuations

I have already emphasised that the NM-M transition is well separated from the critical point in alkali - alkali halide solutions. Chieux *et al.*[37] have investigated the critical behaviour of K-KBr by small-angle neutron scattering near the critical point, lying in this system at a critical temperature T_c = 1000.6 ± 0.1 K and a critical metal concentration $c_c = 0.44$. A critical behaviour of the 3D Ising type was observed for the correlation length and for the susceptibility over a substantial range of reduced temperature. This is consistent with the fact that this system at the critical point, with an electric conductivity close to $10^3\ \Omega^{-1}\ cm^{-1}$, lies well in the metallic regime where the Coulomb interactions are fully screened by conduction electrons.

3.5 Cesium iodide - iodine solutions

As can be seen from figure 1 for the cesium-iodine system, a transition from an ionic to a molecular state occurs in the iodine-rich part of the phase diagram at standard pressure. A NM-M transition may also be expected on this side at higher pressure, according to the discussion given in § 2.3. Rather little is known about this region of the phase diagram.

From measurements of magnetic susceptibility Nakowsky *et al.*[38] have shown that a paramagnetic species appears in the liquid Cs-I system on increasing the iodine content above stoichiometry. This is proposed to consist of I_2^- molecular ions. Upon further increase of iodine content an equilibrium between paramagnetic and diamagnetic species is indicated by the data, the most likely reaction being proposed as $I_2^- + (n-1/2)I_2 \Leftrightarrow I_{2n+1}^-$. Diamagnetic polyiodides are believed to predominate in iodine-rich solutions.

4. Solutions of metals in polyvalent metal halides

A rich variety of melting mechanisms and liquid structures has been identified in the halides of polyvalent metals (for a recent review see Tosi *et al.*[39]). A broad correlation between the structural behaviour of the pure molten salt and the electrical transport in metal solutions can be recognized from the electrical conductivity data reported in the review of Bredig[1]. For instance, the conductivity in Ca-CaX_2 systems (X denoting Cl, Br or I) increases much more slowly with metal content than in Sr-SrX_2 and Ba-BaX_2: this correlates with the fact that the liquid structure of $CaCl_2$ is intermediate in character between the loose ionic structures of $SrCl_2$ and $BaCl_2$ and those of network-forming melts such as $ZnCl_2$. Naturally, electron localisation should be stronger if it requires substantial local reconstruction of a molten salt structure with an appreciable connectivity of its own. Eventually, as one proceeds through polyvalent metals along a path of increasing chemical activity such as that proposed by Pettifor[40], electron localisation by reconstruction of chemical bonding will result. As an example one may mention the Hg-$HgCl_2$ system: this may be viewed as a nonmetallic mixture of $HgCl_2$ and Hg_2Cl_2 in the composition range up to the monohalide Hg_2Cl_2 and as a Hg-Hg_2Cl_2 solution at still higher metal concentration[1, 4]. The stability of such lower oxidation states for a polyvalent metal broadens the nonmetallic range and shifts the liquid-liquid miscibility gap towards to metal-rich side of the phase diagram.

I shall limit the discussion below to the Bi-Bi halides and to cryolite-sodium solutions, as illustrative examples having the special reasons of interest that I have already mentioned in § 1.

4.1 Solutions of bismuth in bismuth halides

The liquid Bi-BiX_3 systems (with X = Cl, Br or I) have been studied extensively from the late fifties[1,2,4,41,42]. The most prominent solid state compounds in the phase diagram are the monohalide and the trihalide. In the latter the Bi^{3+} ions form a layer-type sublattice by occupying octahedral holes in the X^- sublattice. Among the monohalides only for solid BiCl does the structure seem to be known: the tendency of bismuth to form polyatomic clusters is revealed in it by the presence of the Bi_9^{5+} ion in the shape of a unicapped square antiprism. Various other charged Bi clusters are reported to be present in solutions of Bi in eutectic salt mixtures or in aluminates[2]. Neutron diffraction data on liquid Bi-BiI_3 at six compositions were interpreted as giving evidence for preference of Bi-Bi near neighbours and formation of clusters of Bi above the liquidus temperature near the composition corresponding to BiI[43].

From optical absorption studies Boston and coworkers[44] reported that in the dilute metal regime the data could be interpreted by assuming the presence of Bi^+ ions in the solution, whereas two or more Bi associates appeared in more concentrated solutions. In electromotive force measurements[45] it was found that two electrons per BiX_3 molecule are transferred in the dilute metal regime, increasing up to eight electrons in more concentrated solutions. This and other evidence indicates that in salt-rich Bi-BiX_3 solutions the monomer Bi^+ is in equilibrium with one or more polyatomic species. The stability of Bi^+ with respect to Bi^{2+} in very dilute solutions could be attributed to the large gain in polarization energy for the Bi^+ and Bi^{3+} pair relative to two Bi^{2+}[42].

All these solutions exhibit regions of liquid-liquid immiscibility and the chloride and bromide solutions have the additional property of retrograde solubility near the $c = 0.5$ composition: a homogeneous solution will separate into two phases on heating and become again homogeneous on further heating. This is most easily understood as due to a change in liquid structure with temperature, dissociation of the polyatomic species being a possibility[4]. The two-phase region shrinks under pressure and disappears at about 1.6 GPa[46].

The role of polyatomic species in suppressing electronic conductivity is especially evident in the retrograde region of the phase diagram of the chloride and bromide solutions. At temperatures above

T_c and in comparison with alkali halides the electrical conductivity is down by about one order of magnitude in the pure salt, increases slowly with metal content up to $c \approx 0.3$ and rather more rapidly in the range $0.4 \leq c \leq 0.6$. A continuous NM-M transition is occurring in this range of composition, possibly near its upper end where σ approaches the values attained in K - KCl near $c \approx 0.25$.

4.2 Solutions of sodium in cryolite

Molten cryolite (Na_3AlF_6 or $AlF_3 \cdot 3NaF$) corresponds to a stoichiometric compound in a continuous range of liquid $(AlF_3)_c \cdot (NaF)_{1-c}$ mixtures. The Raman scattering spectra of these and other mixtures of AlF_3 with alkali fluorides indicate a gradual conversion of tetrahedral $(AlF_4)^-$ groups into octahedral $(AlF_6)^{3-}$ groups as the mixture becomes more basic with c decreasing below 0.5[47]. At $T \approx 1053$ K and in the range $1/4 \leq c \leq 1/2$ the relative concentration of the latter species is only slightly below the ideal upper limit $(1 - 2c)/2c$ allowed by the available number of fluorines, indicating that each $(AlF_6)^{3-}$ group is essentially free in the liquid rather than part of a fluorine-sharing network. The ionic equilibrium between the two species as a function of composition is well understood theoretically[48] on the basis of a balance between the difference in their binding free energies *in vacuo* and the change in excess free energy of the liquid mixture on dissociation of $(AlF_6)^{3-}$ into $(AlF_4)^-$ and two F^-.

Experiments aimed at clarifying the roles of Al and Na in the cathodic processes involved in the industrial production of Al metal from electrolytic baths containing cryolite were carried out by Grjotheim[49] and Haupin[50]. Grjotheim exposed molten cryolite to Na vapours and reported that, after prolonged annealing followed by cooling into a frozen state, specks of Al metal were deposited in the salt matrix. He also enquired about the origin of the so-called "metal mist" and emission of gas bubbles which occur on adding various metals to molten cryolite. In later experiments Haupin reached the conclusion that on adding Al metal the metal mist forms in the presence of moisture and consists of hydrogen bubbles containing small partial pressures of AlF, $NaAlF_4$ and Na.

A relevant theoretical study of the processes occurring on adding Na metal to molten cryolite was carried out by Akdeniz and Tosi[51]. It was found that electrons are transferred from Na to Al in the melt, with formation of Al^{2+} and Al^+ ions in reduced valence states and enhancement of the $(AlF_4)^-$ structural units. More precisely, their microscopic calculations show that, with increasing content of added Na metal and assuming that this ionises into Na^+ ions and electrons, the

equilibrium between $(AlF_6)^{3-}$ and $(AlF_4)^{-}$ is shifted in favour of the latter. At the same time some of these groups are broken up, releasing into the melt Al^{3+} ions which become available as traps for the chemical binding of the valence electrons. Except for a narrow range of stability of the Al^{2+} ions at high dilution of the added metal, the most stable species are the Al^{+} ions in a monovalent state. These results are fully consistent with the aforementioned observations of Grjotheim and Haupin.

7. Summary and concluding remarks

Studies of molten salts over the last three decades have emphasised two general facts: (i) the connection between the structure of the melt near freezing and that of the hot solid, with regard to short-range charge ordering and to liquid-state traces of the native point defects; and (ii) the wide mutual solubility of different molten salts, often accompanied by structural reconstructions as, for instance, the formation of complex ions in fluoroaluminates. These two themes also underlie the discussion of the atomic and electronic structure of metal - molten salt solutions.

The optical absorption associated with a solvated electron in a molten alkali halide can be usefully related to the F-centre absorption spectra in the solid phase. At variance from the solid, however, the molten salt can dissolve metal over the whole range of composition up to the pure liquid metal. This allows one to follow the evolution of the electronic and ionic structure across the NM-M transition and to enquire about the interplay between this transition and liquid-liquid phase separation. An example of related physical behaviours is offered by the Cs-Au alloy, which near stoichiometry shows structural features reminiscent of molten salt ordering and non-metallic electrical transport properties[5].

The role of compounds formed by cations in reduced-oxidation states and of complex polyatomic cations enriches the behaviour of solutions involving polyvalent metals. The specific example of metal-cryolite solutions is illustrative of what one may expect to be a rather general feature of electron localisation in strongly structured molten salts: electron localisation involves structure breaking and the required expense of free energy is balanced through the reconstruction of the chemical bond. The Bi-Bi halide solutions, on the other hand, are an outstanding example of equilibria involving complex cations - with parallels in the so-called Zintl ions in alloys of alkali metals with group-IV elements[5].

REFERENCES

[1] M. A. Bredig: *Molten Salt Chemistry*, ed. M. Blander, Interscience, New York, 1964, 367.

[2] J. D. Corbett: *Fused Salts*, ed. B. Sundheim, McGraw-Hill, New York, 1964, 341.

[3] N. F. Mott: *Metal-Insulator Transitions*, Taylor & Francis, London, 1974.

[4] W. W. Warren Jr.: *The Metallic and Nonmetallic States of Matter*, ed. P. P. Edwards and C. N. R. Rao, Taylor & Francis, London, 1985, 139.

[5] M. Rovere and M. P. Tosi: *Rept. Progr. Phys.*, 1986, **49**, 1001.

[6] L. Landau and G. Zeldovitch: *Acta Phys. Chem.*, 1943, **18**, 1940.

[7] F. Hensel and H. Uchtmann: *Ann. Rev. Phys. Chem.*, 1989, **40**, 61.

[8] W.-C. Pilgrim, R. Winter and F. Hensel: *J. Phys.: Condens. Matter*, 1993, **5**, B183.

[9] F. Hensel and M. Yao: *Elementary Processes in Dense Plasmas*, ed. S. Ichimaru and S. Ogata, Addison-Wesley, Reading, 1995, 295.

[10] H. Endo and M. Yao: *Elementary Processes in Dense Plasmas*, ed. S. Ichimaru and S. Ogata, Addison-Wesley, Reading, 1995, 307.

[11] K. Tamura and S. Hosokawa: *J. Phys.: Condens. Matter*, 1994, **6**, A241.

[12] V. F. Kozhevnikov, D. I. Arnold and S. P. Naurzakov: *J. Phys.: Condens. Matter*, 1994, **6**, A249

[13] H. G. Drickamer: *Solid State Physics*, 1965, **17**, 1.

[14] O. Shimomura, K. Takemura, Y. Fujii, S. Minomura, M. Mori, Y. Noda and Y. Yamada: *Phys. Rev.* B, 1978, **18**, 715.

[15] M. Pasternak, J. N. Farrell and R. D. Taylor: *Phys. Rev. Lett.*, 1987, **58**, 575.

[16] D. Hohl, V. Natoli, D. M. Ceperley and R. M. Martin: *Phys. Rev. Lett.*, 1993, **71**, 541.

[17] H. Fujihisa, Y. Fujii, K. Takemura and O. Shimomura: *J. Phys. Chem. Solids*, 1995, **56**, 1439.

[18] K. F. Herzfeld: *Phys. Rev.*, 1927, **29**, 701.

[19] P. Ballone, G. Pastore and M. P. Tosi: *J. Chem. Phys.*, 1984, **81**, 3174.

[20] F. Lantelme and P. Turq: *J. Chem. Phys.*, 1984, **81**, 5046.

[21] K. Tankeshwar and M. P. Tosi: *J. Phys.: Condens. Matter*, 1991, **3**, 7511.

[22] K. R. Painter, P. Ballone, M. P. Tosi, P. J. Grout and N. H. March: *Surf. Sci.*, 1983, **133**, 89.

[23] E. Mollwo: *Nachr. Gess. Wiss. Göttingen*, 1935, **1**, 203.

[24] W. Freyland, K. Garbade, H. Heyer and E. Pfeiffer: *J. Phys. Chem.*, 1984, **88**, 3745.

[25] W. W. Warren Jr., S. Sotier and G. F. Brennert: *Phys. Rev. Lett.*, 1983, **50**, 1505.

[26] N. Nicoloso and W. Freyland: *J. Phys. Chem.*, 1983, **87**, 1997.

[27] N. Nicoloso and W. Freyland: *Z. Phys. Chem.*, 1983, **135**, 39.

[28] G. Senatore, M. Parrinello and M. P. Tosi: *Phil. Mag.* B, 1980, **41**, 595.

[29] M. Parrinello and A. Rahman: *J. Chem. Phys.*, 1984, **80**, 860.

[30] A. Selloni, P. Carnevali, R. Car and M. Parrinello: *Phys. Rev. Lett.*, 1987, **59**, 823.

[31] H. J. Yu: Ph. D. Thesis, 1981, University of Chicago.

[32] W. Freyland: *J. Non-Cryst. Solids*, 1990, **117/118**, 613.

[33] I. Webman, J. Jortner and M. H. Cohen: *Phys. Rev.* B, 1975, **11**, 2885.

[34] G. Senatore and M. P. Tosi: *Phil. Mag.* B, 1985, **51**, 267.

[35] D. Yurdabak, Z. Akdeniz and M. P. Tosi: *N. Cimento* D, 1994, **16**, 307.

[36] Z. Akdeniz and M. P. Tosi: *N. Cimento* D, 1996, **18**, 613.

[37] P. Chieux, P. Damay, J. Dupuy and J. F. Jal: *J. Phys. Chem.*, 1980, **84**, 1211.

[38] B. Nakowsky, N. Nicoloso and W. Freyland: *Ber. Bunsenges. Phys. Chem.*, 1984, **88**, 297.

[39] M. P. Tosi, D. L. Price and M.-L. Saboungi: *Ann. Rev. Phys. Chem.*, 1993, **44**, 173.

[40] D. G. Pettifor: *J. Phys.* C, 1986, **19**, 285.

[41] W. W. Warren, Jr.: *Advances in Molted Salt Chemistry*, Vol. 4, ed. G. Mamantov and J. Braunstein, Plenum, New York, 1981, 1.

[42] W. Geertsma and M. P. Tosi: unpublished.

[43] K. Ichikawa and T. Matsumoto: *Phys. Lett.* A, 1981, **83**, 35.

[44] C. R. Boston: *Inorg. Chem.*, 1970, **9**, 389 and references given therein.

[45] J. D. Corbett, F. C. Albers and R. A. Sallach: *Inorg. Chim. Acta*, 1968, **2**, 22 and references given therein.

[46] K. Tamura, H. Hoshino and H. Endo: *Ber. Bunsenges. Phys. Chem.*, 1980, **84**, 235.

[47] B. Gilbert, G. Mamantov and G. M. Begun: *J. Chem. Phys.*, 1975, **62**, 950.

[48] Z. Akdeniz and M. P. Tosi: *Phys. Chem. Liquids*, 1990, **21**, 127.

[49] K. Grjotheim: *Alluminio*, 1953, **22**, 679.

[50] W. E. Haupin: *J. Electrochem. Soc.*, 1960, **107**, 221.

[51] Z. Akdeniz and M. P. Tosi: *Phil. Mag.* B, 1991, **64**, 167.

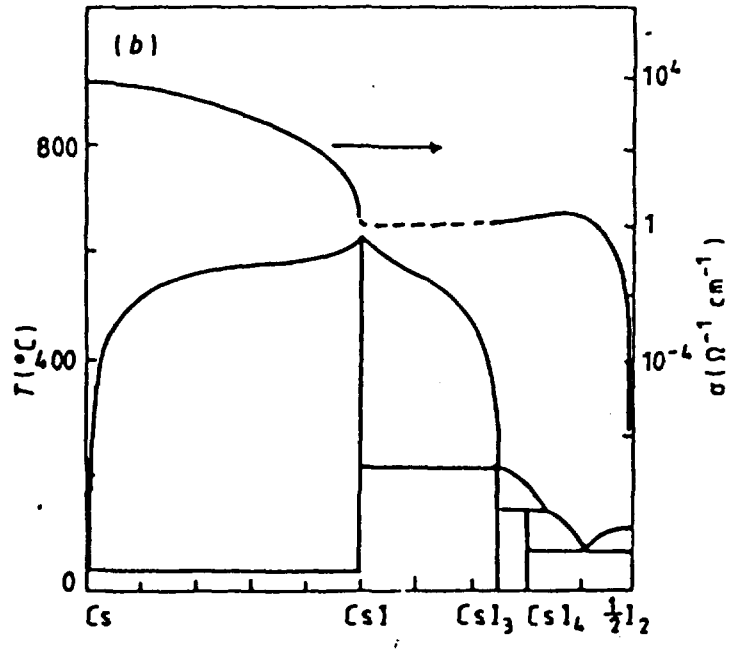

Figure 1. Phase diagram of the cesium-iodine system. The upper curve, with the scale on the right-hand side of the figure, shows the electrical conductivity σ from measurements (full curve) and estimates (broken curve).

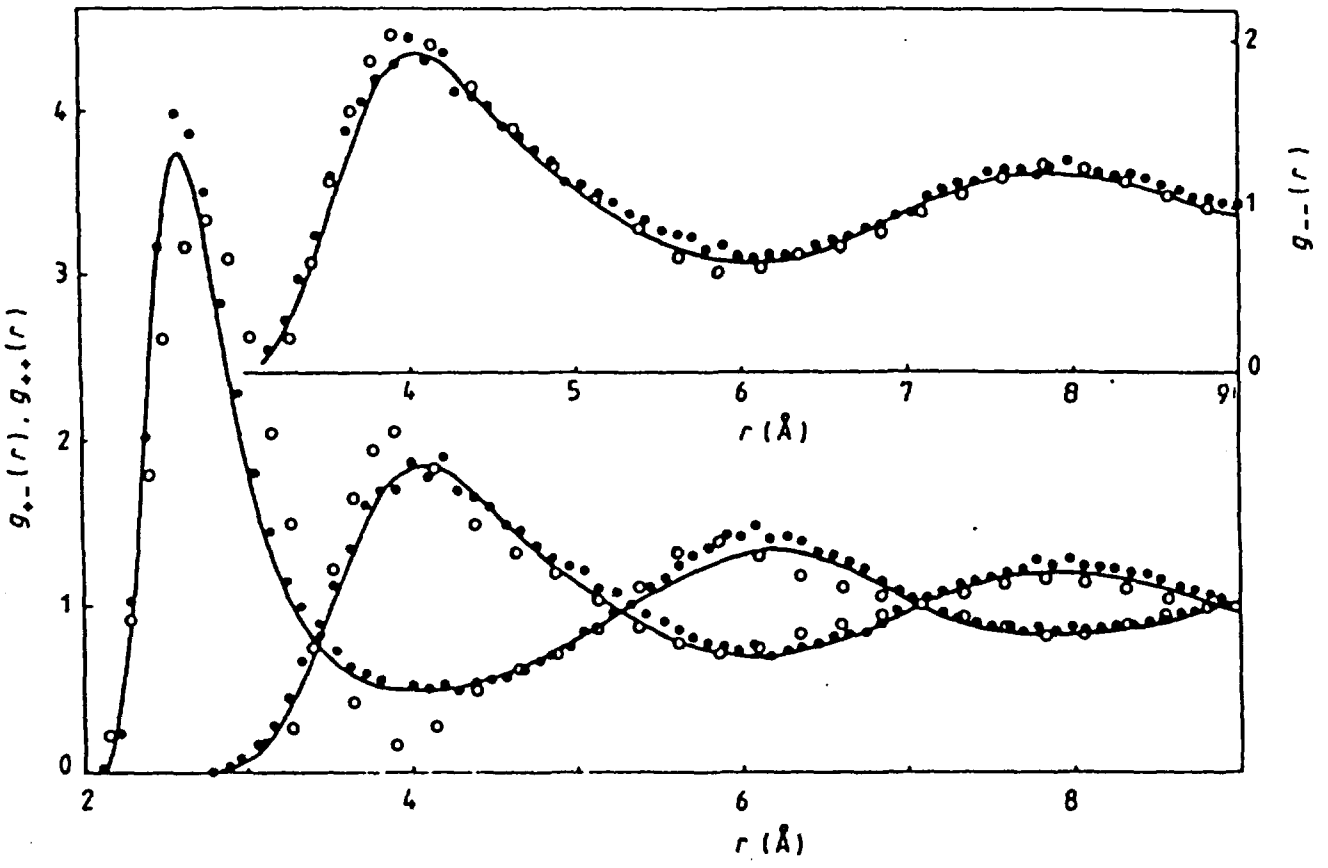

Figure 2. Pair distribution functions of molten NaCl near freezing, from neutron diffraction (circles), computer simulation (dots) and liquid-structure theory (curves).